Square-shaped metal screens in the infrared to terahertz spectral region: Resonance frequency, band gap, and bandpass filter characteristics

O. Sternberg,[1] K. P. Stewart,[2] Y. Hor,[3] A. Bandyopadhyay,[3] J. F. Federici,[3] M. Bornefeld,[4] Y.-L. Mathis,[4] D. Sliwinski,[1] K. D. Möller,[1] and H. Grebel[1,a)]

[1]*Electronic Imaging Center and Electrical Engineering Department, New Jersey Institute of Technology, Newark, New Jersey 07102, USA*
[2]*Naval Research Laboratory, 4555 Overlook Avenue SW, Washington, DC 20375-5351, USA*
[3]*Department of Physics, New Jersey Institute of Technology, Newark, New Jersey 07102, USA*
[4]*Synchrotron Light Source ANKA, Forschungszentrum Karlsruhe, P.O. Box 3640, D-76021 Karlsruhe, Germany*

Resonance frequency of freestanding, square-shaped thick metal screens have been studied here in the wavelength range of infrared (IR) to mm (20 to 0.2 THz). It was found that their peak transmission has a linear relationship to the screen's pitch. An experimental spectral feature, unaccounted for in typical simulations with plane parallel incident beams, was observed in the transmittance envelope for measurements in focused beams. In the past, this spectral feature was assigned to Wood's anomaly. Yet, unlike the latter, the observed spectral feature appears here in the long wavelength regime as well. We investigated this phenomenon for a large frequency range and assigned the spectral feature to the formation of a photonic band gap at oblique incidence. Many IR Fourier transform spectrometers use a noncollimated incident beam and such spectral features will appear whenever the local state of polarization includes components which are parallel to the plane of incidence. © *2008 American Institute of Physics*. [DOI: 10.1063/1.2955765]

I. INTRODUCTION

Freestanding thick metal screens, with a ratio of thickness to periodicity constant larger than 0.1, have been constructed in the short[1] and long wavelength regions.[2,3] Their transmittance was investigated from the visible to the terahertz spectral region due to their important role in astronomy [in particular, infrared (IR) astronomy[4]] and remote sensing. In general, filters are able to discriminate desired IR signals from more energetic short wavelength radiation, allow color temperature measurements, provide order sorting for grating spectrometers, and improve the signal-to-noise ratio of Fourier transform (FT) spectrometers. Square-shaped freestanding metal screens are commercially available and have been used as bandpass filters,[5] reflectors for long IR wavelengths, Fabry–Perot etalons,[6] and antennas.[3]

Previously, most of the application driven spectral investigations were conducted at normal incidence. Interpretation of the transmission data was conveniently made by using a coupled surface plasmon (SP)/wave model.[7,8] In the model, incident light excites a compound mode. The compound mode consists of surface waves on both sides of the screen, which are coupled by waveguide modes in the screen openings.[9–13] One speaks of SPs when the complex refractive index[14] is used and of surface waves when surface impedance boundary conditions[15] are applied. Transmittance through screens is characterized by peak wavelength, peak height, and width. The transmittance depends on geometrical parameters such as screen pitch, size of screen opening, and screen thickness. For example, cross-shaped screens exhibit

one dominant transmission peak with no secondary peak within its envelope. An empirical formula[16] relates the resonance wavelength to the geometrical parameters; simulations with plane waves using a transmission line matrix (TLM) program reproduce the peak wavelength within a few percent.[8]

In this paper we present experimental and simulation results for the transmittance of freestanding square-shaped metal screens with periodicity constants ranging over two orders of magnitude (12.7–1270.0 μm), all having thicknesses around 4 μm. Spectra were taken with blackbody, synchrotron, and terahertz sources. Yet, interpretation of the experimental data in terms of the modes, described above, presents a problem in our case. Simulations with a plane parallel incident wave at normal incidence exhibited only one dominant transmission peak while two peaks were observed experimentally. In the past, minima within the peak envelope have been assigned to Wood's anomaly.[17,18] Wood's anomaly, though, is a diffraction phenomenon where a high order of diffraction propagates at grazing angle with respect to the screen. As such, it is limited to wavelengths *shorter* than the periodicity pitch.[19] Here we reconsider screen features to be much smaller than the incident wavelength (the long wavelength regime) and propose that the split in the transmission peak is related to a photonic band gap, which opens up between two standing waves (two resonance modes). Such modes are typically excited by a *p*-polarized incident beam and *should not* appear when the screen is excited by plane parallel light at normal incidence. In order to maximize their throughputs, most IR spectrometers are constructed with a focused rather than collimated incident beam on the sample. Splitting in the transmission peak appears whenever the incident beam is not collimated. If the incident

a)Electronic mail: grebel@njit.edu.

TABLE I. Screen parameters.

(L/in)[a]	(g)[b]	(L)[c]	Wn[d]	(THz)[e]	WL[f]	Formula: 075g+05L
2000	12.7	7.6	666.7	20.00	15.0	13.33
1500	16.4	11.2	476.2	14.29	21.0	17.90
1000	25.4	18	354.6	10.64	28.2	28.05
750	33.9	25.1	264.6	7.92	37.8	37.98
500	50.8	39.4	177.3	5.32	56.4	57.80
400	63.5	49.3	140.8	4.23	71.0	72.28
200	127.0	106.7	69.4	2.08	144.1	148.60
55	461.8	367	19.7	0.59	507.6	529.83
40	635.0	559	14.0	0.42	714.3	755.75
20	1270.0	1178	6.7	0.20	1492.5	1541.50

[a]Lines/in.
[b]Periodicity constant.
[c]Length of square opening.
[d]Resonance frequency in wavenumber.
[e]Resonance frequency in terahertz.
[f]Resonance wavelength in micrometers. All screens are $3-5$ μm thick.

beam is collimated, then the transmittance dip only appears at oblique incidence.

II. EXPERIMENT

Freestanding, square-shaped, electroformed nickel screens are commercially available from Buckbee–Mears. The screens, designated by their number of lines per inch, geometrical parameters, peak wavelength, and resonance data are compiled in Table I. Blackbody, synchrotron, and terahertz sources were used in this spectral study. We used Brucker IFS 66v/S and Mattson Galaxy FTIR spectrometers with room temperature detectors to study screens 200, 400, 500, 1000, 1500, and 2000 (Fig. 1). Multiple screens 2000 and 750 were studied at noninterference separations. Screens 55, 40, and 20 were studied with blackbody radiation using the Brucker IFS 66v/S FTIR spectrometer with a He-cooled detector, with the synchrotron light source ANKA at the Research Center Karlsruhe in Germany, and with a terahertz source equipped with room temperature detectors [(Picometrix T Ray-2000™ terahertz system) available at NJIT (Fig. 2).

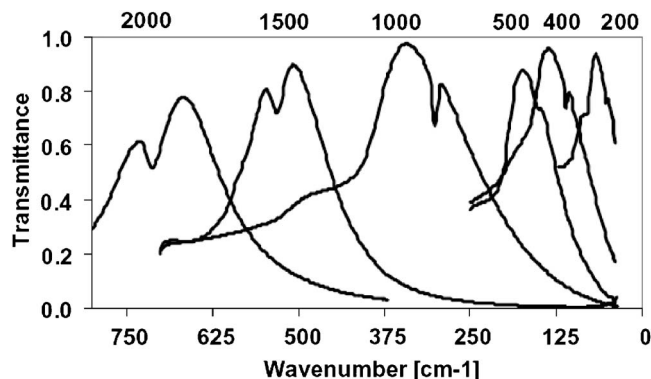Far-IR (FIR) FT spectrometers employing blackbody radiation sources typically use a large input solid angle to increase their throughput, and consequently, their signal-to-noise ratio. The instrument is designed such that the product of area and solid diverging angle is maintained constant (beam area × solid angle=constant) throughout the spectrometer. As a result, a certain fraction of the incident beam remains noncollimated. The synchrotron radiation and the terahertz source of the T Ray-2000™ system are better collimated than the beam generated by a blackbody source. In addition, T Ray-2000™ produces more output power than the other two systems, which allows shorter measurement times. Air was taken as reference. An aluminum aperture of 7 mm diameter was used for all samples. The spectral resolution was 1/80 THz.

III. THEORETICAL CONSIDERATIONS

We consider incident light impinging on a periodic freestanding metal screen of periodicity g at oblique incident angle θ (Fig. 3). Rectangular coordinates x and y are assumed for the screen surface. The plane of incidence is defined by the incident beam direction and the normal to screen surface and its projection follows the x direction. We define the p polarization for electrical vectors that are in the plane

FIG. 1. Transmittances of nickel screens of 2000, 1500, 1000, 500, 400, and 200 lines/in. obtained with Brucker FIR spectrometer at diverging incident angle of 17°.
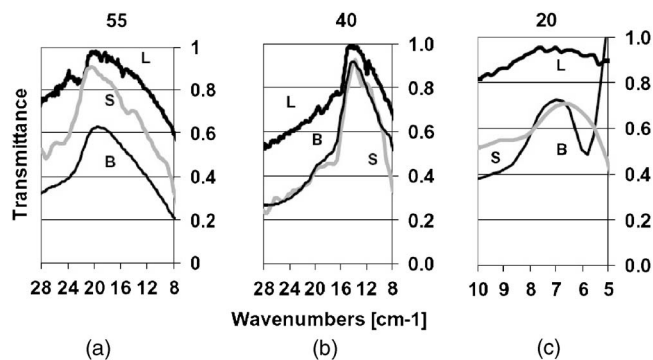

FIG. 2. Transmittances of nickel screens of 55, 40, and 20 lines/in. obtained with blackbody, synchrotron, and terahertz laser radiation. Blackbody (thin black) and synchrotron (gray) radiation were made by using Brucker FIR spectrometer at a nonstandard position where the beam is most collimated (right after the system interferometer). The terahertz laser source (thick black) had a beam width of 7 mm.
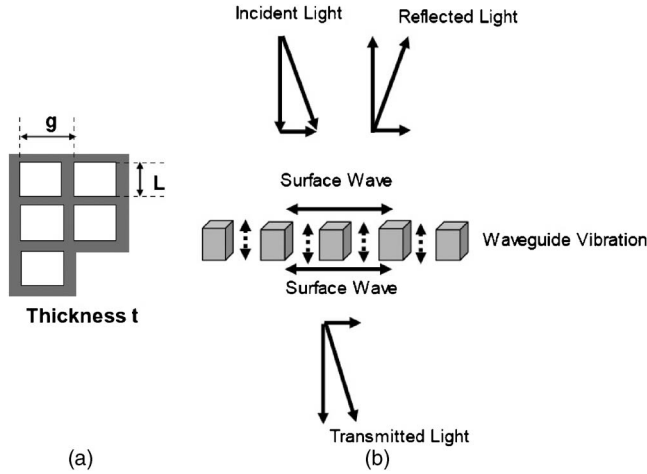
FIG. 3. Incident, transmitted, and reflected light. (a) Schematic of a square-shaped structure. (b) Incident light excites on the front side surface waves, coupled by vibrations to the backside, and leaving the screen in direction of the transmitted light, in a similar process as for reflection on the front side.

of incidence and *s* polarization when the electrical vector is normal to it.[20] A compound mode is excited within the metal screen. Surface waves on both sides of the screen are coupled by waveguide modes in the screen openings. The rectangular channels (waveguides) support TM modes for incident *p* polarization and TE modes for incident *s* polarization. The transmitted and reflected beams are a combination of standing and propagating waves, and are schematically shown in Fig. 3.

Let us consider the projection of an incident beam that propagates along the *x* direction, $k_{0x}=k_0 \sin(\theta)$. The *k* vector of the surface wave propagating at the air/metal boundaries is written as $k_s=k_0(\varepsilon_m\varepsilon_0/\varepsilon_m+\varepsilon_0)^{1/2}$, with ε_m as the dielectric constant of metal and ε_0 as the dielectric constant of air. When considering an ideal metal, $\varepsilon_m \ll 0$, and therefore $k_s \sim k_0$. The coupling to a surface wave takes place via the periodic structure with pitch *g*, at angle θ. Therefore, the excited surface wave along the *x* direction has a propagation constant of, $k_{sx}=k_0 \sin(\theta)+q2\pi/g$, where $q=\pm 1, \pm 2, \ldots$. The frequency is defined as $\omega=\omega(k_{sx})=c[k_0 \sin(\theta)+q2\pi/g]$. The values of $\omega(k)$ in the extended Brillouin zone and truncated zone (gray area) are schematically shown in Fig. 4. We use the light line $\omega=ck_0$ for dispersion relations. The remain-
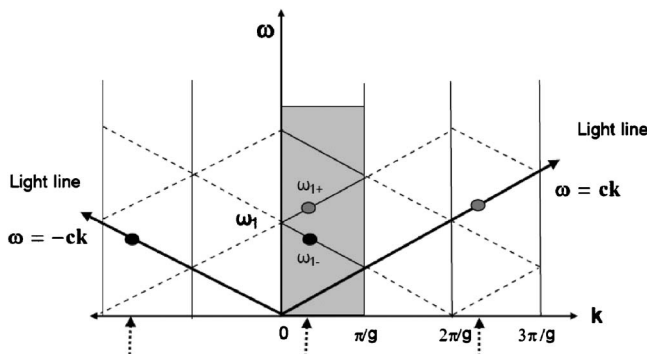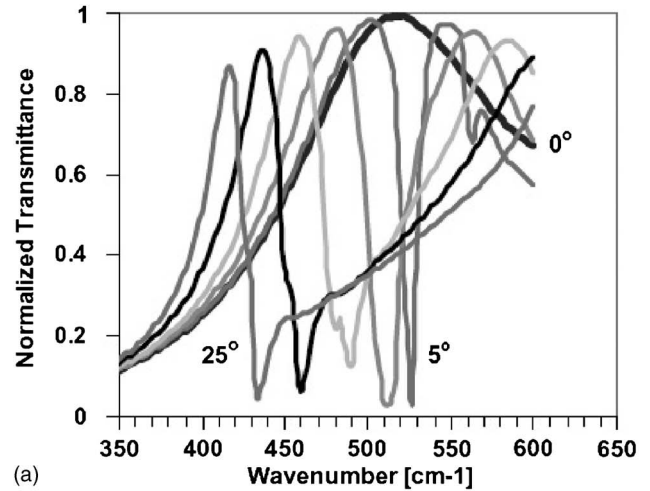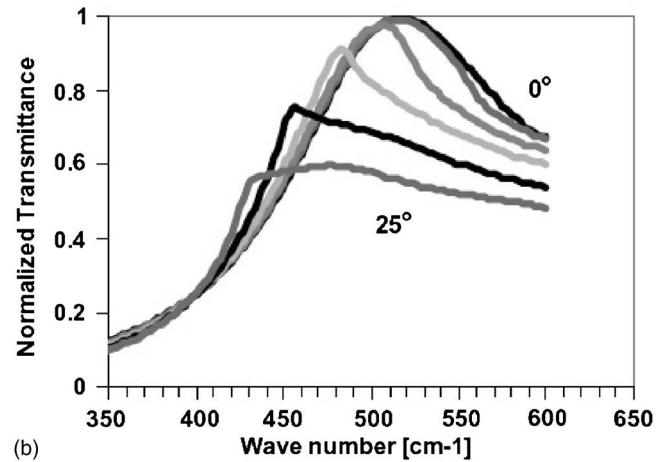

FIG. 4. Dispersion relation $\omega(k)$ (*p* polarization) schematically in an extended Brillouin zone diagram with the $\omega(k)$ values in each zone obtained by folding over the light line $\omega=ck$. We have indicated equivalent k_S values, such as $+2\pi/g +(\omega/c)\sin(\theta)$ and $+2\pi/g -(\omega/c)\sin(\theta)$.

FIG. 5. Simulations with HFSS: Transmittance of *s*- and *p*-polarized beams for screen 1500 at angles 0°, 5°, 10°, 15°, 20°, and 25°. (a) *p* polarization. (b) *s* polarization.

ing projection of the incident beam is a standing wave whose electric field is oscillating parallel to the screen surface (and therefore, may be also called the longitudinal optical mode). The light line, $\omega=ck_0$, determines the corresponding frequencies in the extended Brillouin zone for k_{sx}, $(k_{sx}:[-\pi/g,\pi/g])$. The light line itself indicates the limiting values for the resonance frequencies for this one-dimensional case. There are two frequencies associated with a given launching angle θ: these are ω^- and ω^+ corresponding to k_{sx}^- and k_{sx}^+, respectively. The difference frequency $\Omega=\omega_1^+-\omega_1^-$ defines a frequency gap. At normal incidence, $\theta=0$, the incident beam generates two counterpropagating surface waves, $k_{sx}=\pm q2\pi/g$, and the gap disappears. It has fourfold degeneracy; two opposite components, each along the *x* and *y* directions, respectively.

The effect of the geometrical shape of the openings may be represented by the transfer function $H(g,L,t)$, where *L* is the opening dimension and *t* is the thickness of the screen. For the metal screens we then have $k_s=(\omega/c)H(g,L,t) \times(\varepsilon_m\varepsilon_0/\varepsilon_m+\varepsilon_0)^{1/2}$ and the resonance frequency ω maybe approximated accordingly. Yet, for *thick screens*, the situation is far more complex and requires solution of the full wave equation. Calculations of ω_1^+ and ω_1^- were made by solving Maxwell's equations with the appropriate boundary
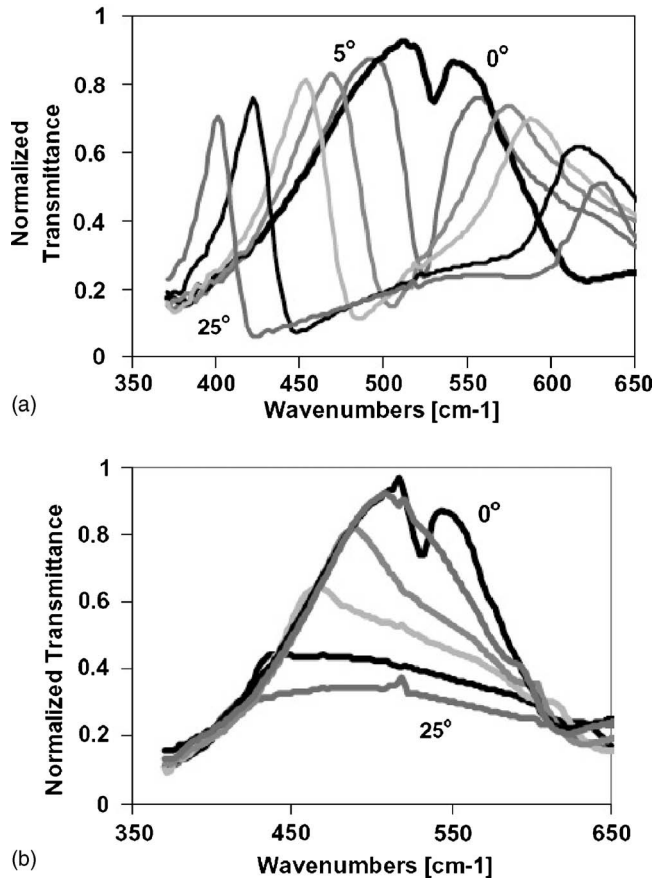
FIG. 6. Experiments: Transmittance of *s*- and *p*-polarized beams for screen 1500 at angles 0°, 5°, 10°, 15°, 20°, and 25°. (a) *p* polarization. (b) *s* polarization.

conditions as made with the Fourier modal method[8] or by using space harmonics.[9] In this paper, we use the TLM method for normal incidence and the Ansoft HFSS package for oblique incidence.

IV. DISPERSION RELATIONS FOR Ω^+ AND Ω^-

Analysis for collimated beams at oblique incidence was made using Ansoft HFSS program. We explored screen 1500 at incident angles of 0° through 25°, both for *s* and *p* polarizations (Fig. 5). Only the *p*-polarization component exhibited peak splitting at incidence angles of 5°–25° (that is, all but the normal incidence case). Experiments corroborating the simulations were made with the Brucker spectrometer. Linearly polarized light, incident at 0° through 25°, with either *s* or *p* polarization was used (Fig. 6). There is good agreement between experiments and simulations for oblique incidence; peak splitting is observed for the *p* polarization but not for the *s* polarization.[21] In Fig. 7, we plot the dispersion relations for experimental and simulated data with both polarization states. A frequency gap is exhibited for *p* polarization, but not for *s* polarization. However, experimental data for normal incidence exhibit a dip in the peak envelope for both polarizations while the simulations do not.

We repeated the simulations with screens 500, 1000, and 1500 at normal incidence using the TLM program, assuming a plane parallel incident beam (Fig. 8). A single transmission
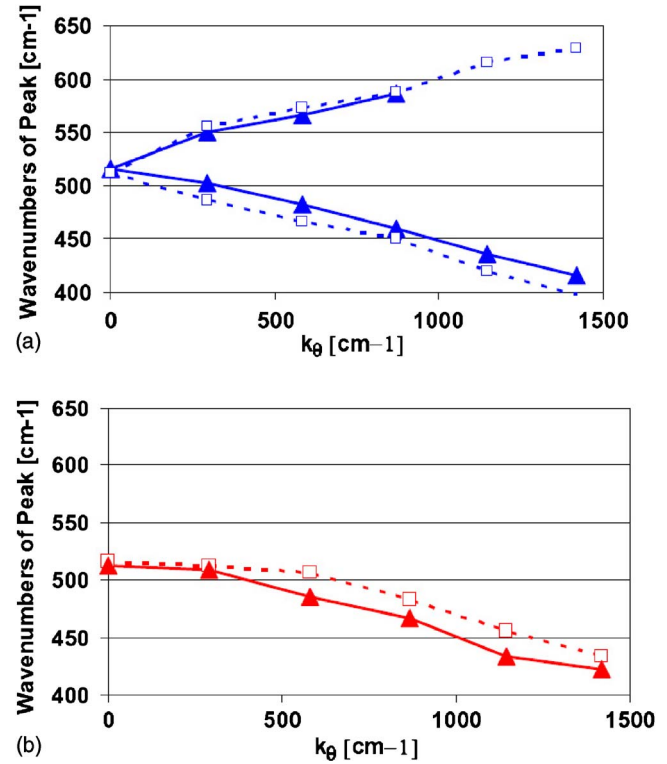

FIG. 7. (Color online) Dispersion relations as peak frequency [cm^{-1}] vs $k_\theta = k_o \sin(\theta)$ for *s*- and *p*-polarized beams for screen 1500 at angles of 0°–25°. Experiments: solid lines. Simulations: Broken lines. (a) *p* polarization. (b) *s* polarization.

peak is exhibited throughout the entire bandpass spectral region unlike the experimental data. Experimental results obtained with terahertz source with screen 55 at normal incidence (Fig. 9) exhibited a dip in the transmittance spectra as well.

Our hypothesis is that the split in the experimental transmission peak is due to the existence of local *p*-polarized component in the incident beam. IR FT spectrometers em-
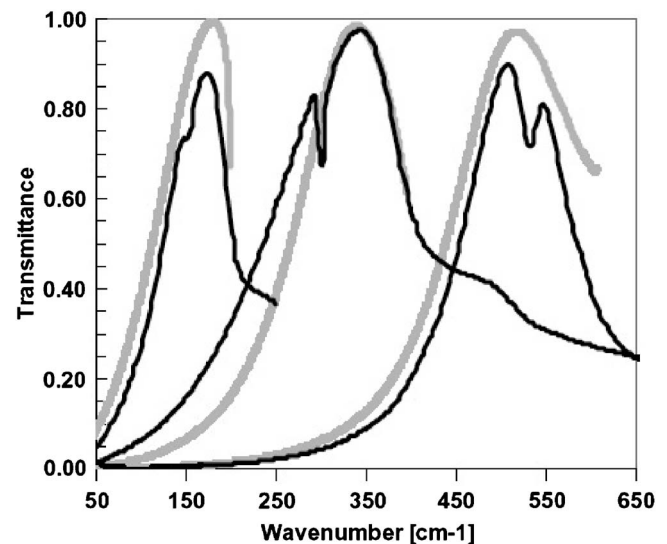

FIG. 8. Transmittance of nickel screens of 500, 1000, and 1500 lines/in. (black) obtained with Brucker FIR spectrometer at converging incident angle of 17°. (Gray) Simulations at normal incidence, assuming plane parallel beam.
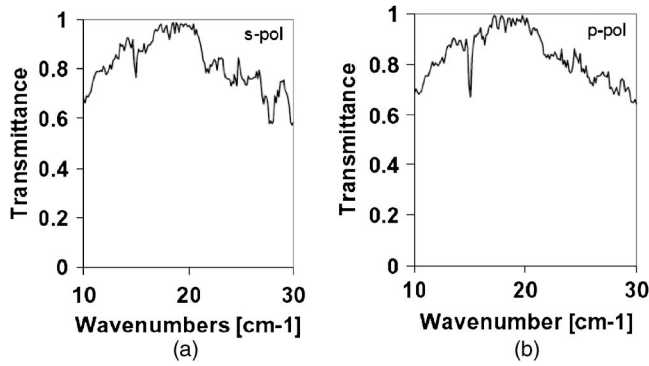
FIG. 9. Experiment with laser light: Transmittance of *s*- and *p*-polarized beams for screen 55 at normal incidence. (a) *s* polarization. (b) *p* polarization.

FIG. 11. Transmittance of one screen 2000. (Black) Brucker FIR spectrometer with 17° cross section opening angle at sample area. (Gray) Mattson near IR spectrometer with $3°-5°$ cross section opening angle at sample area.

ploy extended sources and large *f* numbers to obtain sufficient throughput. Thus, a fraction of the beam is diverging even at normal incidence. Local states of *p* polarization may be identified for each of the azimuthal angles (Fig. 10). This is true for linearly *p*-polarized components at oblique incidence as well. This hypothesis is supported by transmittance studies for the same screen (2000) using two IR spectrometers with different *f* numbers. The Bruker FTIR has an $f/3.3$ beam in the sample chamber. Therefore, each measurement was done not at a single angle of incidence θ, but rather for the range of angles $\theta \pm 8°$. This focused beam differs from the plane wave used in the numerical calculations and must

be taken into account when comparing theory and experiment. The Mattson and Picometrix systems had a better collimated $f/12$ beam. The transmittance becomes a single peak when measured using spectrometer with the larger *f* number, i.e., the spectrometer having the smaller beam solid angle incident on the sample (Fig. 11). Further support was obtained from transmittance measurements of two screens and three screens placed apart at noninterference distances. The transmittance of one, two, and three screens (750) show successive reduction of transmittance [Fig. 12(a)], while two screens placed at an angle show a third peak on the long wavelength side [Fig. 12(b)] as expected (Fig. 6).
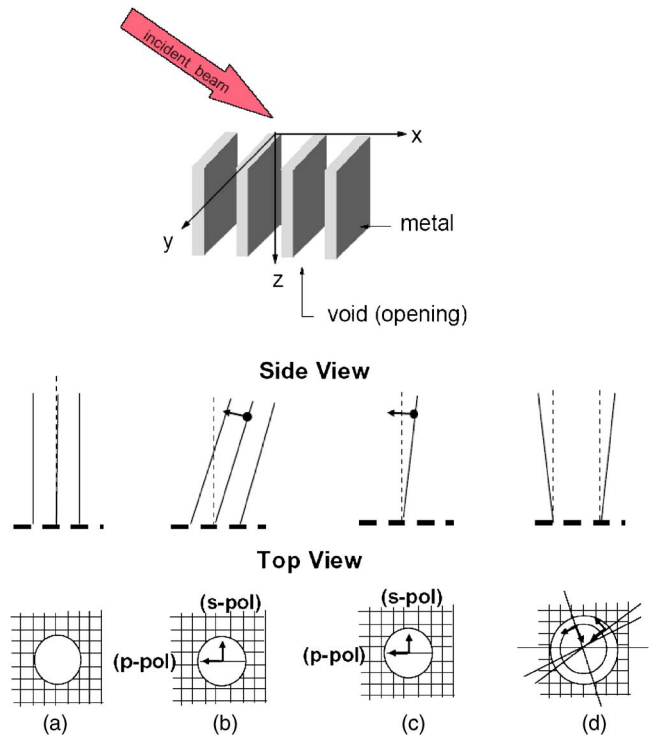

FIG. 10. (Color online) Schematic of experimental and simulations setup with respect to polarization: (a) Simulations with collimated incident beam at normal incidence. (b) Simulations with collimated incident beam at oblique angle, *p* and *s* polarizations with respect to the plane of incidence. (c) The same as (b) for the fraction of noncollimated light at an azimuthal angle. (d) At normal incidence, the same as (c) for a number of azimuthal angles.
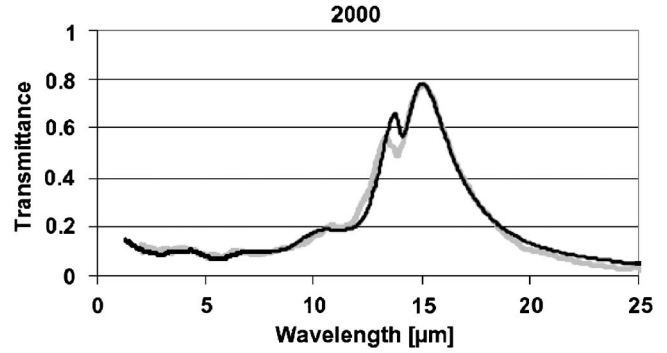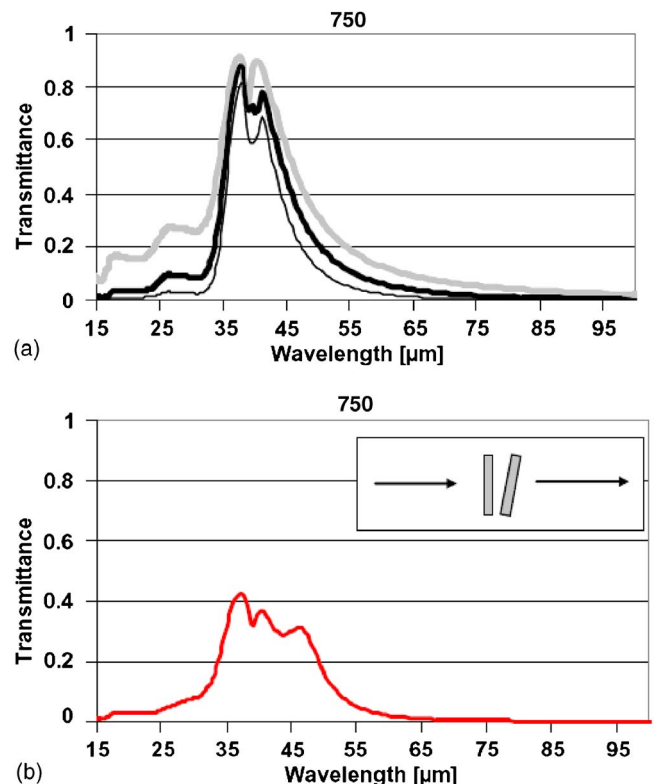

FIG. 12. (Color online) Transmittance of several 750 screens. (a) (Gray) One screen. (Bold black) Two screens. (Black) Three screens. (b) Two screens at an angle of 15°.
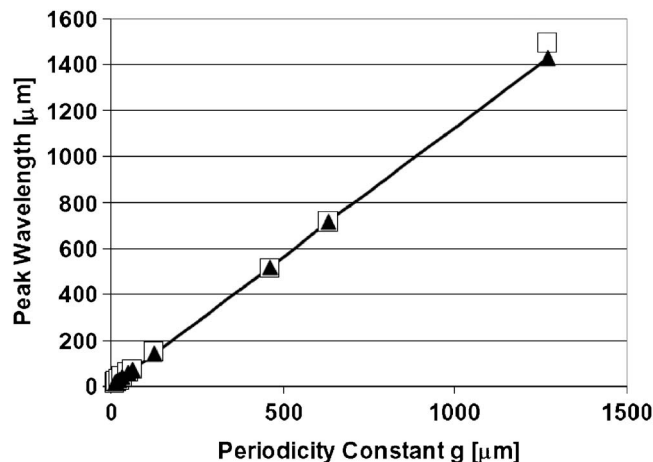
FIG. 13. Phenomenological assessment: Peak resonance wavelength as a function of periodicity constant g. (White square) Experiment. (Black triangle) Empirical formula. The formula is $\lambda_P = 0.75g + 0.5L$ at fixed $L/g = 0.75$, where λ_P is the wavelength corresponding to peak frequency, g the periodicity constant, and L the length of the square opening.

V. PEAK RESONANCE FREQUENCY AND EMPIRICAL FORMULA FOR 20 TO 0.2 THZ RANGE

The spectra depicted in Figs. 1 and 2 exhibited a bandpass response over a large range of periodicity constants: from 12.7 to 1270 μm. The overall bandpass envelope, though, is split by a dip in the transmission curve. The transmission envelope peak is assigned to the resonance frequency ω_P for the $k_s = 0$ mode at normal incidence. The corresponding resonance wavelength λ_P depends linearly on periodicity constant g and length of opening L. An empirical formula $\lambda_P = 0.75g + 0.5L$ for $(L/g = 0.75)$ represents well the experimental data over two orders of magnitude of the periodicity constant. The values of the empirical formula are listed in Table I and plotted in Fig. 13. The dependence of the resonance wavelength on L at a given value of g was also calculated using the TLM program, and the results are plotted for $L/g = 0.6$, 0.75, and 0.9 in Fig. 14. Screens 2000 to 200 exhibited a small modification (albeit linear) to the empirical resonance wavelength value when the opening to periodicity ratio deviated from 0.75.

VI. DISCUSSION

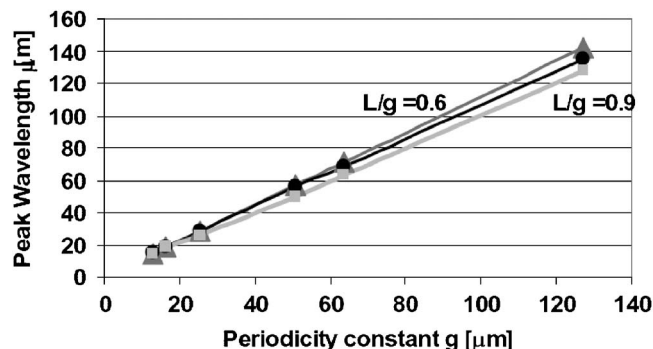Despite attracting renewed interest in recent years, the scattering problem by subwavelength screens dates back to

FIG. 14. Simulations: Peak resonance wavelength as a function of g and L. (Dark gray triangles) $L/g = 0.6$. (Black circles) $L/g = 0.75$. (Light gray squares) $L/g = 0.9$.

the 1960s. While many competing claims have been made in the past, the transmission of screens in the long wavelength region at normal incidence seems to stem from a standing wave resonance close to the SP waves, which is coupled by the modes within the screen openings. The frequency of the resonating waves is obtained from the solution of the wave equation and the periodic boundary conditions. Degeneracy occurs at normal incidence, which is partially removed at oblique incidence. Then, two resonant frequencies appear.

We set to explore the transmission through thick metallic screens at oblique incidence for an extremely broad range of frequencies using several sources and systems. The transmittance of square-shaped metal screens, 2000 to 200 lines/in., exhibited a split transmission envelope; the dip appeared for some screens on the short wavelength side and for others on the long wavelength side (Fig. 1). To a limited extent, other recent investigations also found split transmission features[22–24] without fully considering its polarization aspect, or correlating the appearance with the nature of the beam incident on the sample in the spectrometer used. A similar feature at $\lambda/g > 1$ has been observed in the past on screen 500,[17] and was assigned to Wood's anomaly. However, being of diffractive nature, Wood's anomaly is restricted to the spectral region of $\lambda/g \leq 1$.

Typical spectrometers in the IR wavelength region always have a fraction of noncollimated incident beam at the sample holder position. In a focused beam, a p-polarized component will always be present at the local plane of incidence regardless of the polarizer used (Fig. 10). While we concentrate on the transmission properties of screens, we ought not to forget their filter characteristics. These may be conveniently modeled by a phenomenological linear relationship with excellent agreement with experiment, spanning over many decades of frequencies (Figs. 10 and 13).

VII. CONCLUSION

We have investigated bandpass filters made of thick metal screens. The experimental data exhibited a peak transmission split. Through experiments and simulations, we have established that this peak split occurs for the p-polarized component of the incident beam at oblique incidence. An empirical formula has been developed for the peak transmission wavelength of square-shaped screens.

[1]D. E. Grupp, H. J. Lezec, T. W. Ebbesen, K. M. Pellerin, and T. Thio, Appl. Phys. Lett. **77**, 1569 (2000).
[2]R. Ruprecht, W. Bacher, P. Bley, M. Harmening, and W. K. Schomburg, KfK-Nachr. Jahrg. **23**, 2 (1991).
[3]B. J. Munk, *Frequency Selective Surfaces* (Wiley, New York, 2000).
[4]M. Rebbert, P. Isaacson, J. Fischer, M. A. Greenhouse, J. Grossman, M. Peckerar, and H. A. Smith, Appl. Opt. **33**, 1286 (1994).
[5]G. M. Ressler and K. D. Möller, Appl. Opt. **6**, 893 (1967).
[6]R. Ulrich, K. F. Renk, and L. Genzel, IEEE Trans. Microwave Theory Tech. **11**, 363 (1963).
[7]C.-C. Chen, IEEE Trans. Microwave Theory Tech. **21**, 1 (1973).

[8] K. D. Möller, O. Sternberg, H. Grebel, and P. Lalanne, J. Appl. Phys. **91**, 1 (2002).

[9] R. Ulrich, *Modes of Propagation on an Open Periodic Waveguide for the Far Infrared*, Microwave Research Institute Symposia Series (Polytechnic, Brooklyn, NY, 1974), Vol. XXIII.

[10] L. Martin-Moreno, F. J. Garcia-Vidal, H. J. Lezec, K. M. Pellerin, T. Thio, J. B. Pendry, and T. W. Ebbesen, Phys. Rev. Lett. **86**, 1114 (2001).

[11] W. L. Barnes, W. A. Murray, J. Dintinger, E. Devaux, and T. W. Ebbesen, Phys. Rev. Lett. **92**, 107401 (2004).

[12] K. J. Koerkamp, S. Enoch, F. B. Segerink, N. F. Van Hulst, and L. Kuipers, Phys. Rev. Lett. **92**, 183901 (2004).

[13] W. Fan, S. Zhang, B. Minhas, K. J. Malloy, and S. R. J. Brueck, Phys. Rev. Lett. **94**, 033902 (2005).

[14] H. Raether, *Surface Plasmons on Smooth and Rough Surfaces and on Gratings* (Springer-Verlag, Berlin, 1988).

[15] J. D. Jackson, *Classical Electrodynamics*, 2nd ed. (Wiley, New York, 1975).

[16] K. D. Möller, J. B. Warren, J. B. Heaney, and C. Kotecki, Appl. Opt. **35**, 6210 (1996).

[17] R. C. McPhedran and D. Maystre, Appl. Phys. **14**, 1 (1977).

[18] R. W. Wood, Phys. Rev. **48**, 928 (1935).

[19] H. F. Ghaemi, T. Thio, D. E. Grupp, T. W. Ebbesen, and H. L. Lezec, Phys. Rev. B **58**, 6779 (1998).

[20] S. Ramo, *Fields and Waves in Communication Electronics*, 2nd ed (Wiley, NewYork, 1984).

[21] H. M. Pickett, J. Farhoomand, and A. E. Chion, Appl. Opt. **23**, 4228 (1984).

[22] M. W. Tsai, T. H. Chuang, H. Y. Chang, and S. C. Lee, Appl. Phys. Lett. **88**, 213112 (2006).

[23] D. Van Labeke, D. G'erard, B. Guizal and F. I. Baida, Opt. Express **14**, 11945 (2006).

[24] G. Pisano, P. A. R. Ade, and S. Weaver, Infrared Phys. Technol. **48**, 89 (2006).